A Method for Assessing the Significance of Abnormalities in HMPAO Brain SPECT Images

Alexander S. Houston, Paul M. Kemp and Murdo A. Macleod

Department of Nuclear Medicine, Royal Naval Hospital, Haslar, Gosport, United Kingdom

Methods: A normal atlas for HMPAO rCBF SPECT images was obtained from images of 53 normal controls. Following image registration and normalization, a mean image was extracted, while images representing correlated normal deviants were identified using principal component analysis. These images formed the "building blocks" of the atlas. For subsequent images, the atlas was used to create a "nearest normal equivalent" image, which was compared to a residual standard deviation image to determine the significance of deviations in the new image. **Results:** Images from 30 patients (10 with Alzheimer's disease; 12 with single or multiple infarcts; and 8 normals) were analyzed. **Conclusion:** Using an optimal decision level, 10/10 patients with Alzheimer's disease and 11/12 patients with infarcts were correctly identified, with only one false-positive resulting. We utilized a database of images obtained from normal controls to create a normal atlas.

Key Words: HMPAO brain SPECT; Alzheimer's disease

J Nucl Med 1994; 35:239–244

An atlas of regional cerebral blood flow (rCBF) is generally computed by meaning a series of normal brain images following image registration. A mapping of normal standard deviation (s.d.) or standard error of the mean across the image is then used to test the significance of any deviation in a subsequently obtained image (*1*). This procedure assumes that deviations in normal images are uncorrelated voxel by voxel. There is evidence to suggest that this is not the case for rCBF images (*2*).

Alternatively, rCBF images obtained using single-photon emission computed tomography (SPECT) may be analyzed using a procedure which involves image registration, image normalization and principal components analysis (PCA) (*3*). A previous attempt to apply PCA to planar imaging has been made by Barber (*4*).

Image registration attempts to align anatomical regions on different images by translating and warping image space, while normalization scales images with respect to each other to correct for differences in the acquisition procedure. However, the blood flow distribution itself, taken as a function of anatomical (rather than image) space, is not affected. If variations in this distribution are purely random, a mean image, together with some measure of local variation (such as s.d.), will be sufficient to describe the problem.

Normal variations in the blood flow pattern cannot be handled in this manner since such variation will be correlated from voxel to voxel. This problem requires a method of establishing the nature and significance of correlated normal variants. PCA, using the voxel as a variable, provides a means of identifying such variants in the form of component images (or eigenvectors).

The rationale is to use a database of images obtained from normal controls to create a normal atlas. A mean image and an appropriate set of component images are created forming the "building blocks" of the atlas. These may be combined to create images representing a wide variety of normal patterns. For any subsequent study, the best-fitting normal image pattern may be computed. This pattern is said to represent the "nearest normal equivalent" (NNE) image. The statistical significance of deviations from this image may then be tested.

METHODS

The steps in the analysis are as follows:

1. Acquisition of a series of rCBF images from normal control subjects.
2. Adoption of one of these images as a reference.
3. Registration of each image in the series with the reference image.
4. Normalization of count values in each image with respect to the reference image.
5. PCA applied to the series of registered, normalized images using the voxel as a variable.
6. Formation of a normal atlas consisting of the mean image and a few significant principal component images.
7. Registration and normalization of subsequent images with respect to the reference image.
8. Computation of the NNE image for each subsequent image using the normal atlas.
9. Determination of the statistical significance of deviations from the NNE image.

Database of Normal Controls

SPECT images of rCBF were obtained from 53 normal control subjects. Exclusion criteria included being rendered unconscious

Received Jul. 2, 1993; revision accepted Nov. 4, 1993.

For correspondence or reprints contact: Dr. A. S. Houston, Dept. of Nuclear Medicine, Royal Naval Hospital, Haslar, Gosport, Hampshire, PO12 2AA, United Kingdom.

or concussed, suffering from a neurological illness or participating in boxing or diving.

The acquisition procedure involved an intravenous injection of 600 MBq of technetium-labeled hexamethylphenylineamineoxime (HMPAO) (Amersham International, Ceretec™) performed under controlled conditions. Images were acquired for 15 sec per projection at 64 equal angles of one complete revolution using a gamma camera (Siemens ZLC750) interfaced to a computer (Bartec MICAS V Sun 3/150). The matrix size at acquisition was 64 × 64 with pixel side length equal to approximately 0.6 cm

Image reconstruction is achieved by filtered backprojection using a Shepp-Logan filter with a Hanning window, defined in frequency space by

$$F(\omega) = \frac{\sin(\pi\omega a)}{\pi a}(0.4 + 0.6\cos(2\pi\omega a)),$$

where ω is the frequency space coordinate and a is the pixel side length. This produced 64 axial slice images of 64 × 64 matrix size. In the current study, the images were analyzed without attenuation correction.

Since the brain is seen only in the last 32 slices and, then, only in a quarter of the field of view, a zoomed 32 × 32 × 32 subset of the full image will contain all relevant information while preserving voxel size.

The use of fairly coarse sampling of the image, as well as a backprojection filter with known smoothing properties, is thought to be necessary, since statistical analysis is to be applied to the voxels of the image. For this purpose, other authors have summed count values over the elements of a grid (*5*), effectively smoothing and reducing the spatial resolution of the image.

Image Registration and Normalization

Although image registration and, to a lesser extent, normalization are necessary steps in the procedure, the optimal methods for this application have yet to be established. Presently, the following procedure has been adopted.

Image registration is achieved using 12 degrees of freedom translation and warp (3 degrees for translation, 9 for warp), representing a three-dimensional affine transform (*6,7*). A coordinate transfer function is generated from two images, one of which is taken as a reference. This is then used to translate and warp the space occupied by the other image. The method does not require the use of radioactive markers or the manual definition of fiducial landmarks.

In this study, the image from one of the controls was used as a reference, and all other images in the normal database were registered with respect to it. Subsequent images must also be registered with respect to the reference image prior to analysis.

Normalization is performed on counts in the volume of the cerebellum (*8*). Regions of interest (ROIs) were drawn depicting the area of the cerebellum on each of 12 slices. Since registration has aligned this region for all images, it is a simple task to scale other images to produce the same count value as the reference image. Normalization must be performed on the normal database prior to PCA, and on subsequent images prior to analysis.

Extraction of Correlated Normal Variants

The database of 53 normal control images was used to generate a mean image plus the first few component images. Each image may then be approximated by adding a linear combination of the component images to the mean image. The coefficients required for this combination will vary among the control images and are found during PCA.

Since they are describing variations about a mean image, component images will contain negative, as well as positive, values; in fact, the total count in each component image will be zero. Similarly, for each component, the sum of the coefficients, taken over the control series of images, will be zero. Also, it should be clear that doubling all values in a component image and halving values of coefficients for that image will not affect the image approximation procedure. This allows a degree of freedom which may be used to scale the magnitude of the coefficients. This is done such that the s.d. of the coefficient values, taken over the 53 controls, is fixed at one for each component. The reason for this will become apparent in the next section.

The residual (or deviation) image may be obtained by differencing the original image and its principal component fit (or NNE image). From this, a mapping of s.d. across the image may be computed for normal controls. Note that an appropriate scaling correction must be made for the reduction in degrees of freedom caused by the extraction of components (or common factors).

A mathematical description of the method is given in the Appendix.

Analysis of Subsequent Studies

For rCBF images of subsequent patients, registration and normalization must first be performed. An approximate fit to the new image is then made from the normal atlas using a PCA routine, which determines the optimal (in a least-squares sense) linear combination of component images to add to the mean image. The coefficients used to provide the linear combination are stored for further examination.

Abnormalities in rCBF images are seen as count deficits, i.e., the values of voxels are reduced in such regions. Since only normal images were used in the PCA, it is not expected that abnormal regions will be well represented by the fitting process. For images of normal patients, however, the fitted image should be fairly similar to the original image, assuming that the database of normal controls is representative of the normal population. Since the state of normality is not known a priori, the concept of "nearest normal equivalence" for the fitted image is reasonable.

It is conceivable, however, that a normal variant, taken to the extreme, may produce an abnormal result. It was for this reason that the s.d. of the coefficients of each component was fixed as one for the control series. Coefficient values for images of patients will represent the number of s.d.s in terms of the normal range for the appropriate component. For the purposes of this study, coefficients for these images were constrained to have a limiting value of ±3.

The statistical significance of any deviation between the patient's image and the NNE image is required. This may be found by comparing residual values corresponding to deficits in the patient's image with the s.d. mapping obtained for normal controls. In this way the NNE image replaces the mean image used in conventional analysis.

The Appendix also provides a mathematical description of this procedure.

Preliminary Evaluation Data

The adoption of a gold standard for normality is complicated by the fact that all available normal control studies were included in the database used for extracting the normal variants. This invalidates the subsequent use of these studies (or, indeed, repeated

studies of the same control) for evaluation purposes as bias will be introduced.

Thirty HMPAO studies were selected from patient archives. These corresponded to ten patients with Alzheimer's disease; twelve patients with single or multiple infarcts; and eight patients with no signs of abnormality. For the former two categories, the results were confirmed by other neurological evidence and qualitative and quantitative assessments made by the referring hospital; while, for the latter category, the clinical outcome strongly suggested that the rCBF pattern should be normal. The 30 images were also rated correctly as abnormal or normal by two clinicians working independently in a "blind" trial which included other images. The small number of normal studies results from the exclusion of the control studies and strict exclusion criteria regarding what constitutes normality when patient archives are used.

NNE images were created for all of these, and a statistical analysis of deviations between corresponding image pairs was performed using the method outlined in the last section.

The region of the grey matter was defined by a nuclear medicine physician on the axial slices of the mean image. An abnormality was reported in this region if at least eight connected voxels (chosen to correspond to $2 \times 2 \times 2$ but not necessarily of this geometry) had deficits with respect to the NNE image exceeding a given value (measured in numbers of normal s.d.s). A receiver operating characteristic (ROC) curve based on maximum likelihood estimation (*9*) was formed by combining the abnormal categories and using different s.d. values as decision levels. The area under this curve was computed and used as an index of accuracy. An optimal decision level may be obtained using the Neyman-Pearson objective (*9*) of maximizing the probability of a true-positive while satisfying an upper limit of the probability of a false-positive.

Because of the low number of normals, this was adapted to maximizing the number of correct responses with a fairly lax upper limit of 0.25 on the false-positive rate. A comparison was made, using the same criteria, with the standard technique involving the mean image.

RESULTS

Identification Stage

Image registration, normalization and PCA have been applied to the normal database and a mean image and 20 component images created.

Image registration was fairly successful except at the base of the skull where there remained considerable variation in shape. PCA of the normal database showed that 30.2% of the total variance in the images was contained in the first component, which was almost entirely concerned with resolving this problem.

Until a registration package capable of solving this problem can be implemented, it was decided to omit the bottom eight slices prior to PCA. It was thought that this would have little effect on the management of patients in a nuclear medicine department, since these slices are rarely used in the diagnostic procedure.

The registration and normalization procedure takes around 2 min per image on a computer (Bartec MICAS V Sun Sparc 4/300).

The mean image and the first three component images are shown in Figure 1. The 24 slices are shown from left to right in descending order, beginning at the top of the skull. In the component images, bright areas correspond to positive values and dark areas to negative values.

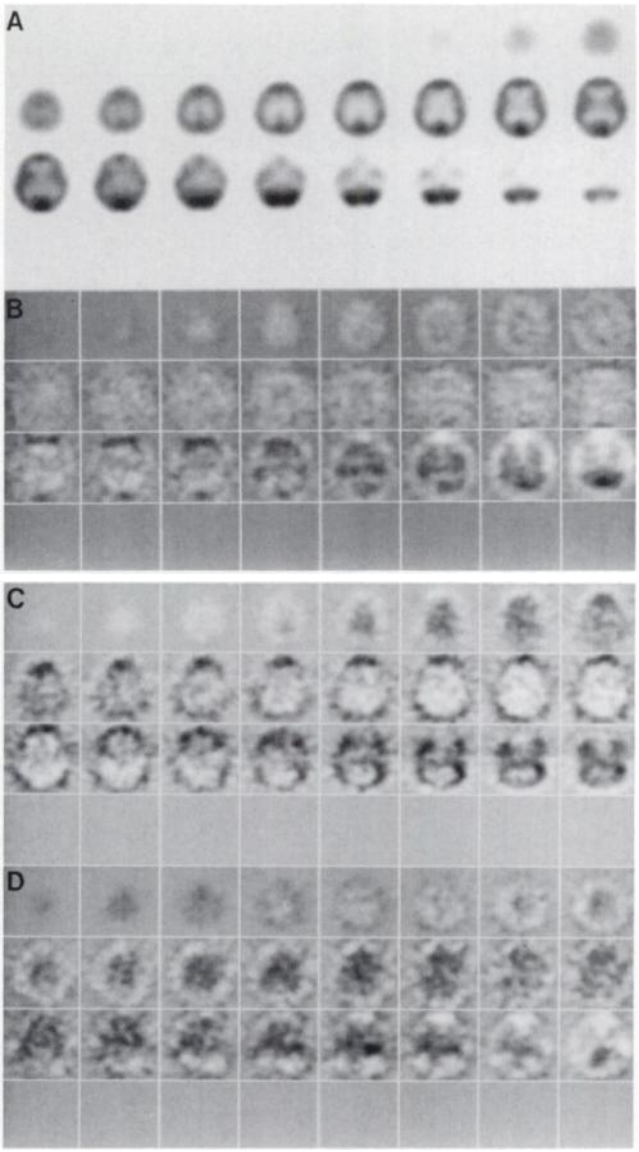

FIGURE 1. Axial slices of (A) the mean image and (B) the first, (C) second and (D) third component images obtained using the 53 normal controls are shown.

The percentage of the total variance remaining after the extraction of each of the first ten components is shown in Table 1. From the total variance an estimate of the (population) count variance in a single image may be made. The expected variance due to noise has previously been estimated as 60.9% of this value using phantom data (*10*). A component may be regarded as significant if the variance remaining after its extraction exceeds that estimated as due to noise. From Table 1 there are seven components which satisfy this condition. In practice it is often wise to stop short of this value, e.g., the presence of nonlinear effects

TABLE 1
Percentage Variance Remaining After the Extraction of Each Component

Component	1	2	3	4	5	6	7	8	9	10
%Variance	89.9	83.0	77.4	72.5	68.2	64.8	61.9	59.3	56.8	54.3

may make the process suboptimal. As a consequence, six components were used for the normal atlas.

PCA, applied to the normal database of 53 controls, takes around 20 min on a computer (Bartec MICAS V Sun Sparc 4/300).

Subsequent Studies

Registration of abnormal images appears to be no more difficult than registration of normal images. For normal images (both within and outwith the control group) the fitted image was generally similar to the original. For abnormal images analyzed subsequently, the region containing the abnormality appeared to be normal on the fitted image. This concurs with the concept of an NNE image.

Figure 2 shows a normal image acquired subsequently together with its NNE image. Figure 3 shows the image pair for a patient with Alzheimer's disease, while Figure 4 shows the image pair for a patient with a large right frontal infarct. In each case, the fitted images appear to be normal while retaining the normal characteristics of the original. In particular, they are different from each other and from the mean image (Fig. 1A). The creation of an NNE image takes around 5 min on a computer (Bartec MICAS V Sun Sparc 4/300).

Evaluation

The number of images in each category reported as statistically abnormal is shown in Table 2. The optimal decision or cut-off level (in s.d.s) is also shown, as is the area under the ROC curve. Specificity and sensitivity at the optimal level are improved when NNE images are used, although a larger sample is necessary to determine the significance of this effect. Note that the optimal decision levels are marginally under 3 s.d.s. This corresponds to a difference of approximately 12%, which is consistent with levels used previously for the detection of an abnormality (*11,12*). The area under the ROC curve is superior when the NNE image is used.

DISCUSSION

The technique of creating an NNE image has initially produced encouraging results. Clearly, a more complete validation of the method using a larger sample is necessary and this is proceeding.

It is of great importance that the series of normal controls is large and varied in parameters such as age. For this reason, the initial image of all normal controls seen in the department was included.

No attenuation correction has been used in this study since, at present, none is used routinely in our department. In order to gauge its effect, the 53 images in the control series were corrected using a standard technique (*13*) and an atlas created as before. The main difference was that only five components were necessary to specify the atlas within noise levels (*10*). It is thought that lack of attenua-

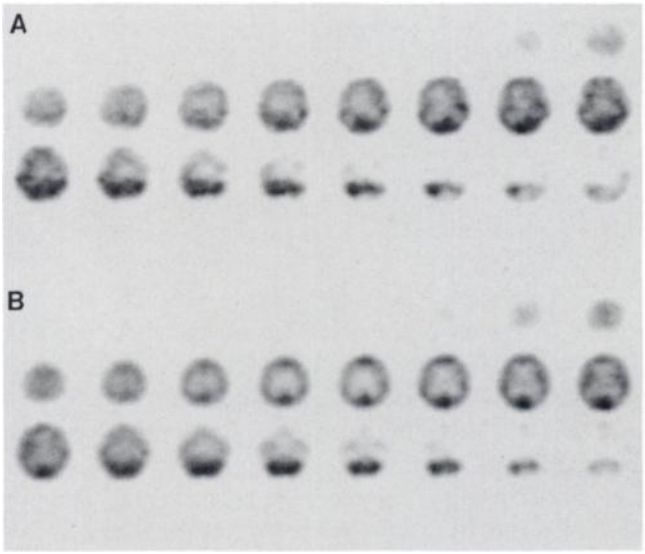

FIGURE 2. Axial slices of (A) the image of a normal patient and (B) the corresponding "nearest normal equivalent" image are shown.

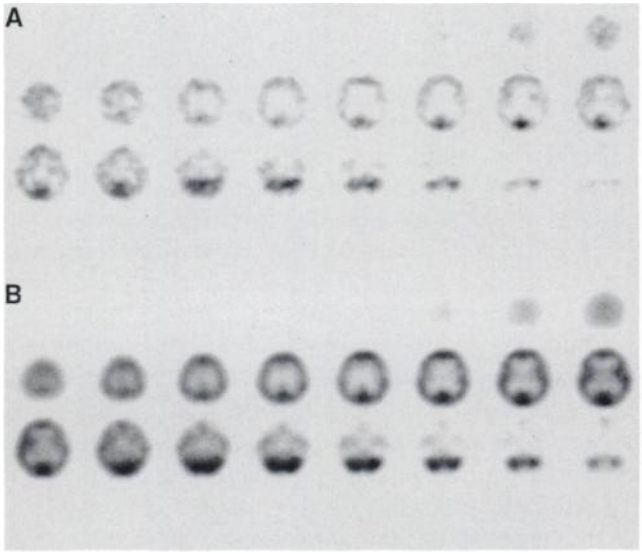

FIGURE 3. Axial slices of (A) the image of a patient with Alzheimer's disease and (B) the corresponding "nearest normal equivalent" image are shown.

tion correction may have a differential effect when brains of different sizes are registered and that the use of one additional component in the computation of the NNE image may compensate for this.

The use of the region of the cerebellum for normalization purposes will not be appropriate in every case, e.g., a stroke patient with crossed-cerebellar diaschesis. For such cases, alternative methods of normalization are currently under review.

The technique is intended to identify and assess both global and regional abnormalities, provided that the latter are sufficiently large enough to be detected in a low resolution image. Generally, the method is equally applicable to high resolution images obtained from multiheaded and annular systems. However, since the registration procedure adopted in this paper is intended for low resolution images, it will be necessary to adopt a more robust procedure for this purpose. A registration procedure involving fiducial markers, e.g., (*14*), would be more suitable.

The use of filtered backprojection and image registration may introduce nonlinear, as well as linear, effects into the images. The method of PCA will handle these in a linear fashion. As a result, such effects will manifest themselves through several components. Although this may make the procedure suboptimal, it is not felt that this, in itself, is a major problem. However, if the component images are contaminated by nonlinear effects, they cannot be interpreted without resorting to some kind of transformation. It is for this reason that no attempt has been made at this stage to interpret these images or to correlate their coefficients with physical parameters such as age. An investigation into the presence of nonlinear correlations in the images is proceeding.

Small lesions have been reported in a few images used in the control series (*12*). These should not affect the first few components of a PCA which will instead reflect normal variations of a more general nature. However, the question of what constitutes a normal rCBF pattern remains. It is hoped that this work represents an important step in the quest for a solution.

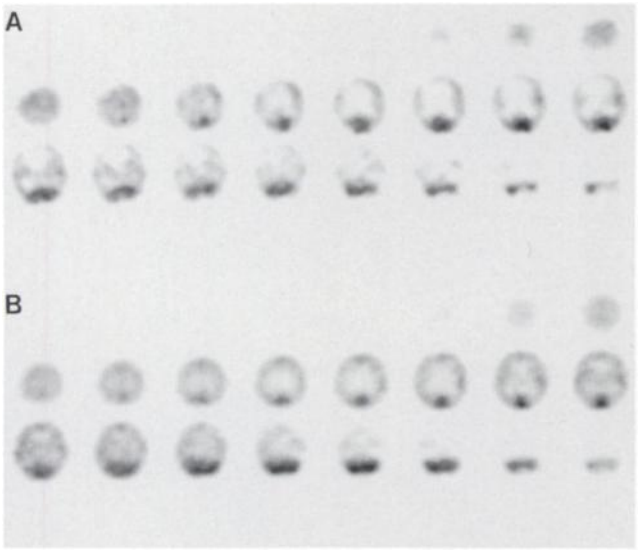

FIGURE 4. Axial slices of (A) the image of a patient with a large right frontal infarct and (B) the corresponding "nearest normal equivalent" image are shown.

TABLE 2
Numbers of Images with Statistically Significant Deficits Found in the Region of the Grey Matter

Method	Cut-off (s.d.s)	Alzh. /10	Inf. /12	Norm. /8	Area under ROC curve
Using NNE	2.9	10	11	1	0.94
Using mean	2.8	10	9	2	0.86

Alzh. = Patients with Alzheimer's disease; Inf. = Patients with infarcts; Norm. = Normal patients.

APPENDIX

Principal Components Analysis Applied to SPECT Images

In the following discussion it will be assumed that all images have been suitably registered and normalized.

Let us assume that we have a set of images $\langle d_j \rangle_i$ for N normal individuals, where d_{ij} is the count in the jth voxel for the ith individual. It is required that each image be approximated by a mean image plus a linear combination of p images each representing some common factor, i.e.,

$$d_{ij} = \bar{d}_j + \sum_{k=1}^{p} w_{ik} c_{kj} + e_{ij},$$

where c_{kj} is an element of $\langle c_j \rangle_k$, the kth common factor image; w_{ik} is the coefficient of this image for the ith individual; and e_{ij} is the error of the approximation. If it is further required that $\sum\sum e_{ij}^2$ is a minimum for a given value of p, the problem reduces to the classical PCA problem (*15*). The coefficients w_{ik} and common factor images $\langle c_j \rangle_k$ (called principal components or eigenvectors and representing correlated normal variants) may be obtained using PCA. These will be unique apart from the fact that, since they form a product, a scaling up of one will be accompanied by a corresponding scaling down of the other. In this case the s.d. (or variance) of the coefficient values is fixed at one for each component, i.e., for each value of k

$$\frac{\sum_{i=1}^{N} w_{ik}^2}{N-1} = 1.$$

The residual variance in voxel j, after the extraction of a mean image and p components, is given by

$$\sigma_j^2 = \frac{\sum_{i=1}^{N} e_{ij}^2}{N-1-p},$$

and a residual s.d. image $\langle \sigma_j \rangle$ may be formed. Note that one degree of freedom is removed for each component extracted.

For a subsequent patient image $\langle g_j \rangle$ the count in the jth voxel may be represented by

$$g_j = \bar{d}_j + \sum_{k=1}^{p} w_k c_{kj} + \varepsilon_j.$$

From PCA, the optimum values of w_k (subject to $|w_k| \leq 3$) required to minimize $\sum \varepsilon_j^2$ may be obtained, producing an image $\langle \hat{g}_j \rangle$ with voxel values given by

$$\hat{g}_j = \bar{d}_j + \sum_{k=1}^{p} w_k c_{kj},$$

which, since $\langle \bar{d}_j \rangle$ and $\langle c_j \rangle_k$ were obtained from a normal database, may be considered to be the NNE image.

The difference image $\langle \varepsilon_j \rangle$ may then be compared to the residual s.d. image $\langle \sigma_j \rangle$ obtained from the normal controls, and a resultant image $\langle -\varepsilon_j/\sigma_j \rangle$ formed. This image will give the significance of a deficit in a voxel expressed in units of the normal residual s.d.

Implementation Note. When the number of variables greatly exceeds the number of individuals, it is desirable to reverse their roles during the initial PCA computation.

ACKNOWLEDGMENT

The authors are grateful to David C. Barber of the Royal Hallamshire Hospital, Sheffield, U.K. for the use of his image registration computer program.

REFERENCES

1. Seitz RJ, Bohm C, Greitz T, et al. Accuracy and precision of the computerized brain atlas programme for localization and quantification in positron emission tomography. *J Cereb Blood Flow Metab* 1990;10:443–457.
2. Bekier A. Does the human brain age asymmetrically?—a hypothesis. *Nucl Med Commun* 1986;7:793–796.
3. Houston AS, Barber DC. Registration of a SPECT brain image with its 'nearest normal equivalent' image. Proc 4th Int Conf on "Image processing and its applications." *IEEE Conf Publ* 1992;354:369–372.
4. Barber DC. Digital computer processing of brain scans using principal components. *Phys Med Biol* 1976;5:792–803.
5. Hooper HR, McEwan AJ, Lentle BC, Kotchen TL, Hooper PM. Interactive three-dimensional region of interest analysis of HMPAO SPECT brain studies. *J Nucl Med* 1990;31:2046–2051.
6. Horn BKP, Schunck BG. Determining optic flow. *Artificial Intelligence* 1981;17:185–203.
7. Barber DC. Registration of low resolution medical images. *Phys Med Biol* 1992;37:1485–1498.
8. Syed GMS, Eagger S, Toone BK, Levy R, Barrett JJ. Quantification of regional cerebral blood flow (rCBF) using $^{99}Tc^{m}$-HMPAO and SPECT: choice of the reference region. *Nucl Med Commun* 1992;13:811–816.
9. Swets JA, Pickett RM. *Evaluation of diagnostic systems: methods from signal detection theory*. New York: Academic Press; 1982.
10. Houston AS, Kemp PM, Griffiths PT, Macleod MA. An estimation of noise levels in HMPAO rCBF SPECT images using simulated and phantom data [Abstract]. *Nucl Med Commun* 1993;14:269.
11. Podreka I, Suess E, Goldenberg G, et al. Initial experience with technetium-99m HMPAO brain SPECT. *J Nucl Med* 1987;28:1657–1666.
12. Kemp PM, Macleod MA, Jenkins L, Houston AS, Toms L. Cerebral perfusion in amateur boxers. Is there evidence of brain damage [Abstract]? *Nucl Med Commun* 1991;12:279.
13. Bellini S, Piacentini M, Cafforio C, Rocca F. Compensation of tissue absorption in emission tomography. *IEEE Trans Acoustics Speech Signal Process* 1979;ASSP-27:213–218.
14. Maguire GQ, Noz ME, Lee EM, Schimpf JH. Correlation methods for tomographic images using two and three dimensional techniques. In: *Medical imaging*. Dordrecht: Martinus Nijhoff; 1986:266–279.
15. Harman HH. *Modern factor analysis*. Chicago: University of Chicago Press; 1976.